



ARTICLE

Enhanced lysosomal function is critical for paclitaxel resistance in cancer cells: reversed by artesunate

Zhe Li¹, Yu-ting Zhu¹, Min Xiang², Jun-lan Qiu³, Shou-qing Luo⁴ and Fang Lin¹

The mechanism underlying the resistance of cancer cells to chemotherapeutic drug varies with different cancer cells. Recent evidence shows that lysosomal function is associated with drug resistance of cancer cells. Artesunate, a derivative of artemisinin, displays broad antitumor activity and direct cytotoxicity on various tumor cells. Our previous study shows that artesunate increases autophagosome accumulation, while significantly decreases autolysosome number in cancer cells, suggesting that artesunate might impair the lysosomal function. In this study, we investigated the effects of artesunate on lysosomal function and its relationship with chemotherapeutic drug resistance in cancer cells. We found that the lysosomal function was significantly enhanced in two drug-resistant (A549/TAX and A549/DDP) cells. Furthermore, we showed that the enhanced lysosomal function by overexpression of transcription factor EB (TFEB) significantly increased MCF-7 cells resistance to doxorubicin (DOX), whereas the decreased lysosomal function by TFEB-knockdown or lysosome inhibitor chloroquine increased MCF-7 cells sensitivity to DOX. Treatment of A549/TAX cells with artesunate (2.5–50 μ M) dose-dependently inhibited lysosomal function and the clearance of dysfunctional mitochondria, and induced cell apoptosis. Moreover, we demonstrated that artesunate exerted more potent inhibition on the resistant (A549/TAX and MCF-7/ADR) cells with higher activity of lysosomal function. Our results suggest that artesunate or other inhibitors of lysosomal function would be potential in the treatment of cancer cells with drug resistance caused by the enhanced lysosomal function.

Keywords: artesunate; cisplatin-resistant human lung adenocarcinoma cells (A549/DDP); paclitaxel-resistant human lung adenocarcinoma cells (A549/TAX); doxorubicin-resistant human breast cancer cells (MCF-7/ADR); lysosome; TFEB

Acta Pharmacologica Sinica (2021) 42:624–632; <https://doi.org/10.1038/s41401-020-0445-z>

INTRODUCTION

A significant barrier to the success of chemotherapy is cancer cells with multidrug resistance, which may be associated with membrane p-glycoproteins, abnormal enzyme activity, anti-apoptosis-related gene expression, and enhanced DNA repair capacity [1, 2]. Some studies have reported that lysosomotropic agents can reverse multiple drug resistance in cells [3, 4]. However, the mechanism is not clear.

In recent decades, research on lysosomes has developed quickly. Lysosomes play important roles in protein secretion, endocytic receptor recycling, energy metabolism, and cell signaling [5, 6]. Lysosomes are acidic membrane-bound organelles found in nearly all animal and plant cells. vATPase can pump protons (H^+ ions) into lysosomes and maintain lysosomes in a steady acidic environment [7]. The pH of lysosomes ranges from 4.5 to 5.0, which is optimal for hydrolysis enzymes, including peptide enzymes, tissue proteases, and phosphatases. Therefore, the lysosome is a critical hub for the turnover and recycling of cellular components, playing a key role in sensing intracellular nutrients in organelles [8–10]. Dysfunctional lysosomes may induce cell death. For example, manzamine A, a

vATPase inhibitor, can inhibit the proliferation of pancreatic cancer cells [11]. In addition, it was reported that protonated drugs with hydrophobic weak bases could be suppressed in lysosomes, preventing drugs from reaching their targets to exert toxicity to cancer cells [12].

Artesunate, a semisynthetic derivative of artemisinin, is a more effective and soluble antimalaria drug than artemisinin, and it is on the essential medicine list of the World Health Organization. Some research has also demonstrated that artesunate has a broad antitumor activity and direct cytotoxicity on various tumor cells [13–15]. Since artesunate has a special peroxide bridge structure and is able to produce reactive oxygen species (ROS), the production of ROS, oxidative DNA damage and sustained DNA double-strand breaks have been reported as potential targets of artesunate in different kinds of tumor cells [16–18]. However, the specific antitumor mechanisms require further research. In our previous research, we found that artesunate increased the number of autophagosomes, while the autolysosome number was significantly decreased in the cells treated with artesunate. This suggests that artesunate might impair lysosomal function [19]. Therefore, in the present study, we tested the effect of

¹Department of Pharmacology, Laboratory of Aging and Nervous Diseases (SZS0703), Soochow University School of Pharmaceutical Science, Suzhou 215123, China; ²Suzhou Vocational Health College, Suzhou 215123, China; ³Department of Oncology, The Affiliated Suzhou Science & Technology Town Hospital of Nanjing Medical University, Suzhou 215123, China and ⁴Peninsula Medical School, University of Plymouth, Research Way, Plymouth PL6 8BU, UK

Correspondence: Shou-qing Luo (shouqing.luo@plymouth.ac.uk) or Fang Lin (bluestonelin@hotmail.com)

These authors contributed equally: Zhe Li, Yu-ting Zhu, Min Xiang

Received: 18 December 2019 Accepted: 15 May 2020

Published online: 23 July 2020

artesanate on lysosomal function and assessed its relationship with cell death.

MATERIALS AND METHODS

Cell culture

A human breast cancer cell line (MCF-7), human cervical cancer cell line (HeLa), human colon cancer cell line (HCT116), human liver cancer cell line (HepG2), and human lung adenocarcinoma cell line (A549) were obtained from the Cell Bank of the Chinese Academy of Sciences (Shanghai, China). A549/TAX cells and A549/DDP cells were purchased from Shanghai Meixuan Biological Science and Technology Co., Ltd. All cells were cultured in Dulbecco's modified Eagle's medium (DMEM) (Gibco) containing 10% fetal bovine serum (FBS) (Gibco) with 100 U/mL penicillin and 100 µg/mL streptomycin. The A549/TAX cells were cultured with 0.2 µg/mL paclitaxel in medium, and the A549/DDP cells were cultured with 0.1 µg/mL cisplatin in medium. The cells were incubated at 37 °C in a humidified atmosphere of 5% CO₂.

Drugs and reagents

Artesunate, trolox (TX), doxorubicin (DOX), and chloroquine (CQ) were purchased from Sigma (St. Louis, MO, USA). Paclitaxel was purchased from Bristol-Myers Squibb (Clinton, N.Y., USA), and cisplatin was purchased from Hanson (Jiangsu Province, China). A cell counting kit-8 (CCK-8) was purchased from Dojindo (Dojindo, Japan). A mitochondrial membrane potential assay kit (JC-1), cell mitochondria isolation kit, Hoechst, and dihydroethidium (DHE) were purchased from Beyotime (Shanghai, China). LysoTracker Red, DQ Green BSA, and LysoSensor Green were purchased from Invitrogen (Carlsbad, CA, USA).

CCK-8 assay

The viability of the cells was determined by CCK-8 assay. The cells (1×10^3) were seeded into 96-well plates and incubated at 37 °C. After 24 h, drugs were added to each well. After 72 h, 10 µL of CCK-8 assay solution (diluted with DMEM containing 10% FBS) was added to each well, and the plate was reincubated for 2 h at 37 °C. The absorbance value (A value) for each well was measured at 450 nm with a microplate reader. The inhibition rate of the cells was determined using the following formula: viability rate (%) = (A value of the experimental group/A value of the control) \times 100%.

Western blot analysis

After being treated with drugs for 24 h, the cells were harvested and dissolved in lysis buffer on ice. Total proteins (~50 µg) from each sample were separated using 10%–15% SDS-PAGE and then transferred onto nitrocellulose filter membranes. After protein transfer, the membranes were blocked for 1 h with 5% nonfat milk at room temperature and then incubated overnight with primary antibodies at 4 °C. The next day, the membranes were washed in TBST (0.1% Tween-20 in TBS) three times (10 min each) and then incubated with secondary antibodies for 2 h. After being washed with TBST buffer, the blotted proteins were detected with an Odyssey infrared imaging system (LI-COR, USA). ImageJ software was used to analyze the results and calculate the expression of the protein.

The following antibodies were used: anti-PARP antibody (#9532, Cell Signaling Technology), anti-Caspase3 antibody (#9661, Cell Signaling Technology), anti-Cytochrome c antibody (#11940, Cell Signaling Technology), anti-Cathepsin B antibody (#C6243, Sigma), anti-Cathepsin D antibody (#SC-377299, Santa Cruz), anti-Cathepsin L antibody (#ab6314, Abcam), anti-P62 antibody (#P0067, Sigma), anti-LC3 antibody (#NB600-1384, Novus Biologicals), anti-TFEB antibody (#4240, Cell Signaling), anti-LAMP1 antibody (#SAB3500285, Sigma), anti-GAPDH antibody (#ab9484, Abcam), anti-COX IV antibody (#11967, Cell Signaling Technology), and anti-β-Actin antibody (#A5441, Sigma).

Gene knockdown and overexpression

Cells were transfected with siRNAs using the RNAiMAX transfection reagent. Single-stranded oligonucleotides (siRNAs) were synthesized by Shanghai GenePharma. The sequence for the siRNA against TFEB was as follows: human 5'-GAGACGAAGGTTCAACATCAA-3'. In addition, an irrelevant oligonucleotide was used as a negative control. The lentivirus-TFEB (LV-TFEB) was established by Shanghai GeneChem (Shanghai, China).

Evaluation of mitochondrial membrane potential

After being treated with a drug for 24 h, the cells were incubated at 37 °C for 20 min with JC-1 fluorescent probe (Beyotime Biotech, China). The supernatant was immediately removed, and the cells were washed twice with PBS and then visualized with a microscope.

Hoechst 33342 staining

After incubation for 24 h, the cells were treated with different concentrations of drugs for 24 h, and the unmodified cell medium was used as a negative control. According to the instructions of the Hoechst 33342 kit, the cells were incubated with Hoechst 33342 for 20 min. The supernatant was immediately removed, and the cells were washed twice with PBS and then visualized with a microscope.

Live cell imaging and quantification of lysosomes

The lysosomal pH was estimated using LysoTracker Red. Cells were grown on glass coverslips in 24-well plates that had been pretreated with 0.01 mol/L poly-D-lysine (PDL). After culturing in medium containing drugs for 24 h, cells at 70%–80% confluence were incubated with 10 µg/mL LysoTracker Red in complete media for 20 min at 37 °C. The cells were washed twice with cold PBS, and the coverslips with cells were mounted with a slide and visualized with a microscope within 10 min.

LysoSensor Green

Cells were grown on glass coverslips in 24-well plates pretreated with 0.01 mol/L PDL. After culturing in medium containing drugs for 24 h, cells at 70%–80% confluence were incubated with 10 µg/mL LysoSensor Green in complete media for 1 h at 37 °C. The cells were washed twice with cold PBS, and the coverslips with cells were mounted onto slides and then visualized with a microscope within 10 min.

DQ Green BSA

Cells were grown on glass coverslips in 24-well plates that were pretreated with 0.01 mol/L PDL. After culturing in medium containing drugs for 24 h, cells at 70%–80% confluence were incubated with 10 µg/mL DQ Green BSA in complete media at 37 °C for 6 h. The cells were washed twice with cold PBS, and the coverslips with cells were mounted onto slides and then visualized with a microscope within 10 min.

Immunofluorescence

Cells were grown on glass coverslips in 24-well plates that were pretreated with 0.01 mol/L PDL. After cultured in medium containing drugs for 24 h, the cells were washed twice with cold PBS and fixed with cold 4% paraformaldehyde for 15 min. Then, the cells were permeabilized with 0.1% Triton X-100 and blocked with 5% FBS for 1 h. The cells were incubated with the primary antibodies overnight and subsequently with the fluorescent secondary antibodies for 1 h followed by DAPI for 10 min. The cells were then washed in PBS, and the coverslips with cells were mounted onto slides and then visualized with a microscope.

Statistical analyses

Data were presented as the means \pm SD and were analyzed using Prism software. All statistical calculations were performed

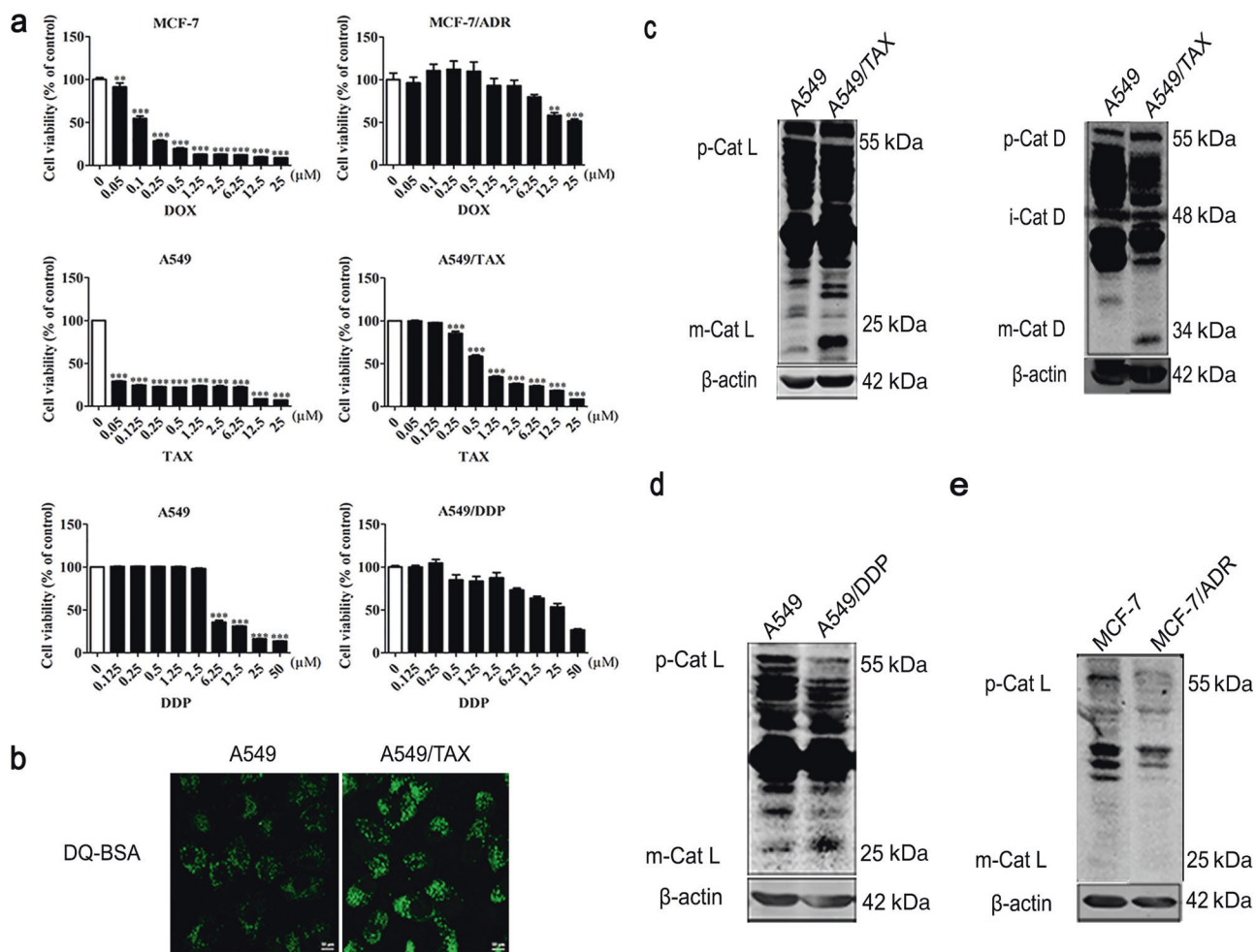


Fig. 1 The activity of lysosomal cathepsins is enhanced in paclitaxel-resistant cancer cells. **a** CCK-8 assay results showing doxorubicin sensitivity of the MCF-7 cells and MCF-7/ADR cells, paclitaxel sensitivity of the A549 cells and A549/TAX cells, and cisplatin sensitivity of the A549 cells and A549/DDP cells. **b** DQ Green BSA fluorescence staining of the A549/TAX cells. **c** Western blot detection of the cathepsin L and cathepsin D levels in the A549/TAX cells. **d–e** Western blot results showing the cathepsin L level in the A549/DDP cells and MCF-7/ADR cells.

using GraphPad Prism software (version 5; GraphPad Software, Inc., La Jolla, CA, USA). Statistical significance was considered when $P < 0.05$.

RESULTS

The activity of lysosomal cathepsins is enhanced in paclitaxel-resistant cancer cells

To explore the mechanisms of chemotherapeutic drug resistance in cancer cells, we selected three different drug-resistant cell lines: cisplatin-resistant human lung adenocarcinoma cells (A549/DDP), paclitaxel-resistant human lung adenocarcinoma cells (A549/TAX) and DOX-resistant human breast cancer cells (MCF-7/ADR). We tested the drug resistance of these three cell lines. After we generated an initial full-range dose-effect curve, we focused our concentration on a narrow data range to obtain a fine-tuned dose-effect relationship (Fig. 1a). We aimed to characterize the pathways that are important to drug tolerance. Therefore, we examined the lysosomal activity in the paclitaxel-resistant cells. DQ Green BSA is a fluorogenic substrate of protease, it brightly fluoresces when the protease reaches an acidic environment, therefore, it was used to test lysosomal activity [20]. Interestingly, DQ Green BSA fluorescence staining showed that the lysosomal activity in the A549/TAX cells was significantly higher than that in the control cells (Fig. 1b). Cathepsin L and D are two important hydrolases in lysosomes, and their mature (cleaved) form can

indicate lysosome function. We determined the activity levels of lysosomal hydrolases and found that the A549/TAX cells exhibited enhanced mature cathepsin L and D activity (Fig. 1c). Similarly, the levels of mature cathepsin L were also increased in the A549/DDP cells (Fig. 1d). In contrast, no significant change in mature cathepsin L level was observed in the MCF-7/ADR cells compared with that in the MCF-7 control cells (Fig. 1e). These data suggest that A549/TAX cells have enhanced levels of lysosome activity, which could contribute to the paclitaxel resistance of the cells.

The transcription factor EB (TFEB) promotes tolerance of cells after drug treatment

TFEB is a prominent regulator of lysosome biogenesis, improving the function of autophagy/lysosomes by regulating the expression of autophagy- and lysosomal-related genes. MCF-7 cells did not exhibit significant tolerance to DOX drug treatment (Fig. 1a), and we asked whether TFEB overexpression can confer enhanced tolerance to DOX treatment on the cells. We established stable TFEB-expressing MCF-7 cells by lentivirus-TFEB (LV-TFEB) infection. TFEB expression was confirmed by immunofluorescence and Western blot assays (Fig. 2a, b). Interestingly, the overexpression of TFEB protein increased both the levels of proenzyme and the mature cathepsin L and those of pro-cathepsin D and mature cathepsin D (Fig. 2c, d). Critically, upon DOX treatment, the LV-TFEB-MCF-7 cells exhibited higher viability than the cells in the control group (Fig. 2e). In contrast, knocking down TFEB

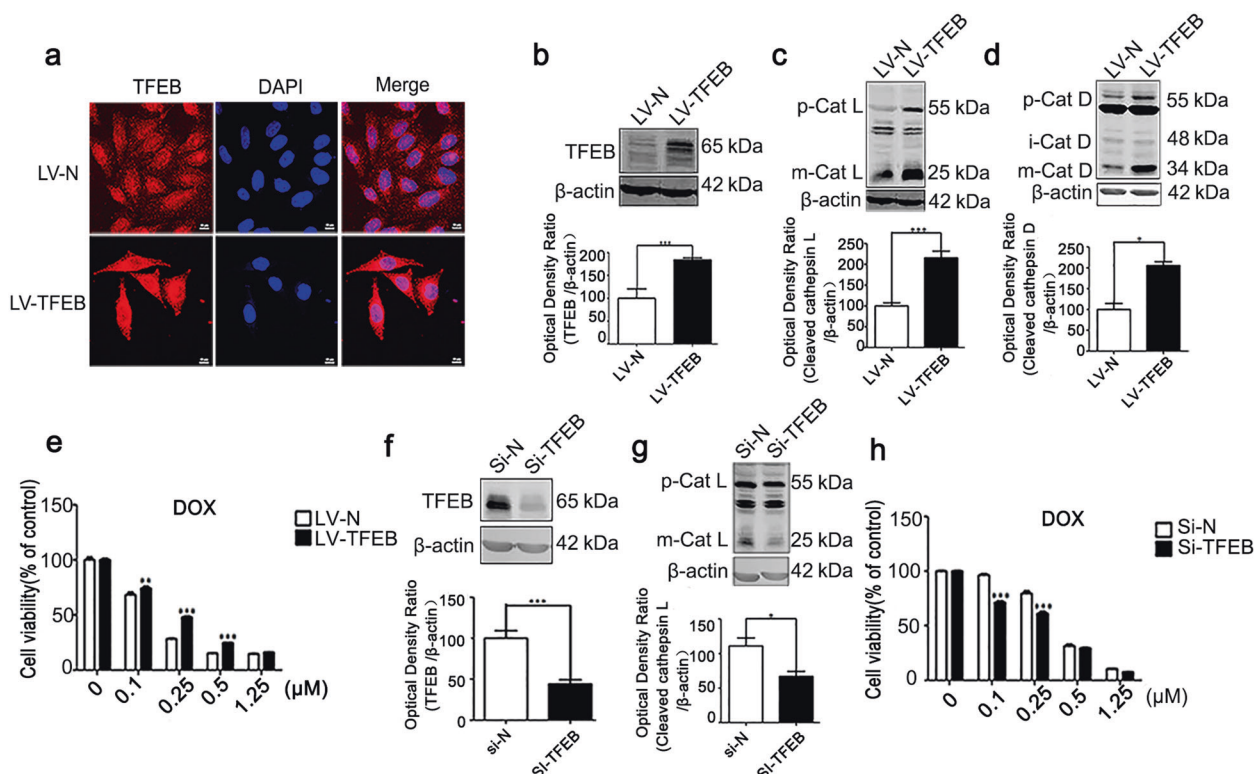


Fig. 2 The transcription factor EB promotes the tolerance of cells after drug treatment. **a** Immunofluorescence staining of TFEB in the LV-TFEB-MCF-7 cells. **b** Western blot detection of TFEB. **c** Western blot detection of cathepsin L in the LV-TFEB-MCF-7 cells. **d** Western blot detection of cathepsin D in the LV-TFEB-MCF-7 cells. **e** CCK-8 assay results showing the proliferation of LV-TFEB-MCF-7 cells treated with doxorubicin for 72 h. **f** Western blot detection of TFEB in the Si-TFEB-MCF-7 cells. **g** Western blot detection of the cathepsin L level in the Si-TFEB-MCF-7 cells. Actin was used as the loading control. **h** CCK-8 results showing the proliferation of the TFEB-knockdown cells treated with doxorubicin for 72 h. Quantitative analysis was performed with ImageJ software. Values are presented as the means \pm SD from three independent experiments. * $P < 0.05$, ** $P < 0.01$, *** $P < 0.001$, and ns $P > 0.05$ versus the control group.

significantly decreased the levels of cathepsins (Fig. 2f, g), and upon DOX treatment, the TFEB knockdown led to decreased cell survival compared with that in the control group (Fig. 2h). These data suggest that the drug tolerance of cancer cells is attributable to lysosomal activation.

Artesunate inhibits the function of lysosomes

Artesunate, as a potential chemotherapeutic drug, has been shown to induce cancer cell death [21, 22]. We confirmed that artesunate inhibited the proliferation of MCF-7 cells (Fig. S1a), HeLa cells (Fig. S1b), HCT116 cells (Fig. S1c), HepG2 cells (Fig. S1d), and A549 cells (Fig. S1e) in a dose-dependent manner. The levels of cleaved PARP were also increased in these cells after artesunate treatment (Fig. S2a), although the levels of RIP1 and RIP3, which are implicated in necroptosis, did not undergo a significant change (Fig. S2b). Consistently, artesunate treatment caused chromatin condensation in MCF-7 cells (Fig. S2c). Previously, we had shown that artesunate impairs autolysosomal function [19]. Therefore, we sought to determine whether artesunate had a direct effect of causing lysosomal dysfunction that is implicated in cell death.

Artesunate treatment significantly decreased the levels of mature cathepsin L and mature cathepsin D in a dose-dependent manner, and it also decreased the levels of mature cathepsin L and mature cathepsin D that had been elevated by DOX (Fig. 3a, b). LysoTracker staining has been widely used to mark lysosomes on the basis of the acidic pH of lysosomes [23]. Artesunate significantly reduced the fluorescence intensity of the LysoTracker stain in the MCF-7 cells (Fig. 3c). The autophagosome fuses with the lysosome to form the autolysosome. The acidic pH

and hydrolases of the lysosome lead to the degradation of the internal membranes of autophagosomes and their contents [24]. Therefore, lysosomal dysfunction causes autophagosome accumulation. Transmission electron microscopy, performed after the experiments were completed, indicated that treatment with artesunate for 24 h induced autophagosome accumulation but decreased the formation of autolysosomes in the MCF-7 cells (Fig. 3d). These data support that artesunate impairs lysosomal function, suggesting a potential role of artesunate in killing drug-tolerant cancer cells. The Western blot results also showed that artesunate obviously increased the expression level of P62, and bafilomycin, an autophagy inhibitor, increased the levels of both LC3 and P62. These data suggest that artesunate blocks autophagic flux (Fig. 3e).

Artesunate inhibits lysosomal function and induces cytotoxicity in A549/TAX cells

We also sought to determine whether artesunate impairs lysosomal function in paclitaxel-resistant cells. Using electron microscopy, we observed significant morphological changes in the A549/TAX cells after 24 h of artesunate treatment, including fewer lysosomes and accumulated dysfunctional mitochondria in the cells (Fig. 4a). In addition, the expression level of LAMP1 decreased while that of P62 increased after artesunate treatment (Fig. 4b). Similarly, the LysoTracker staining results showed that artesunate significantly decreased the fluorescence intensity of the lysosomes in the A549/TAX cells (Fig. 4c). DQ Green BSA fluorescence staining showed that the fluorescence intensity of the A549/TAX cells was decreased with artesunate treatment (Fig. 4d). Moreover, the protein levels of the lysosomal cathepsins,

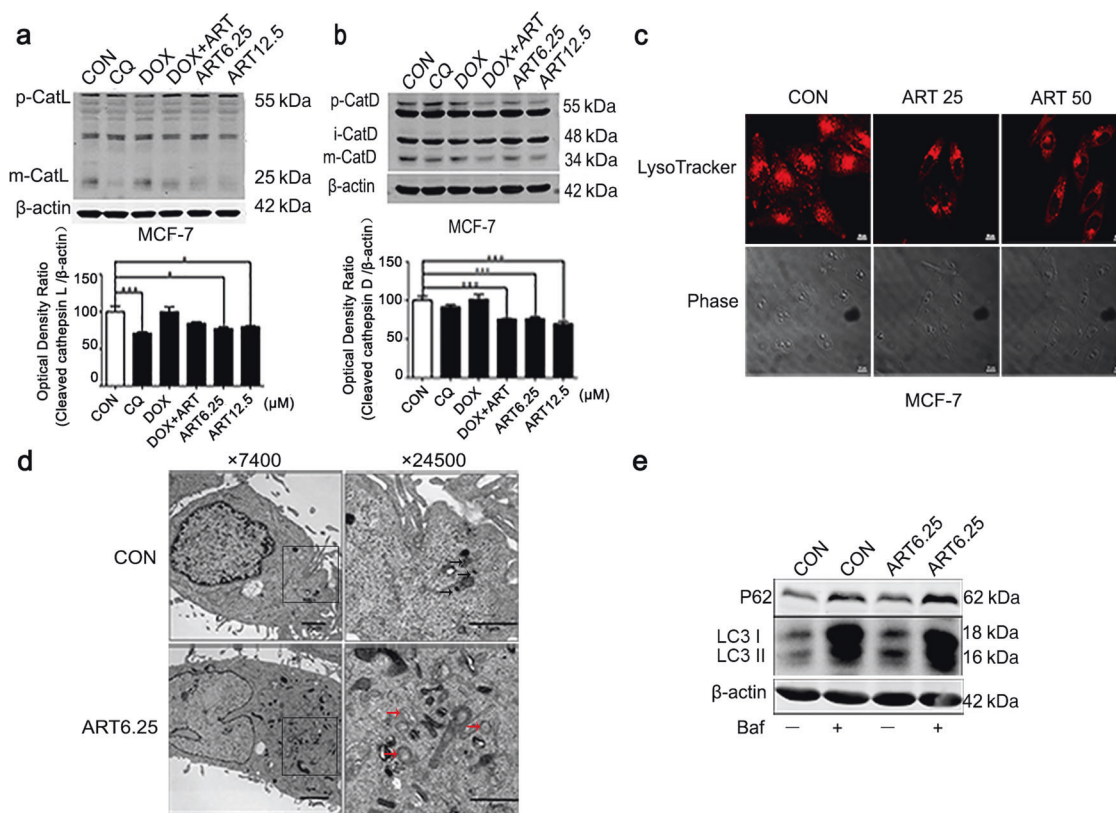


Fig. 3 Artesunate inhibits the activity of cathepsins in MCF-7 cells. **a** Western blot detection of cathepsin L in the MCF-7 cells after treatment with artesunate for 24 h. **b** Western blot detection of cathepsin D in the MCF-7 cells after treatment with artesunate for 24 h. **c** LysoTracker detection in the MCF-7 cells after treatment with artesunate for 24 h. **d** Electron microscopy results showing autophagy in the MCF-7 cells treated with artesunate for 24 h. The black arrow indicates autophagosomes, and the red arrow indicates autolysosomes. **e** Western blot detection of P62 and LC3 in the MCF-7 cells after treatment with artesunate for 24 h in the presence or absence of bafilomycin A1. Actin was used as the loading control. Quantitative analysis was performed with ImageJ software. Values are presented as the means \pm SD from three independent experiments. * $P < 0.05$, *** $P < 0.001$, and ns $P > 0.05$ versus the control group.

including mature cathepsin L (Fig. 4e), mature cathepsin B (Fig. 4f) and mature cathepsin D (Fig. 4g), were reduced after artesunate treatment. These results showed that artesunate inhibited lysosomal function in the A549/TAX cells and caused the aggregation of dysfunctional mitochondria that could not be cleared by lysosomes.

Then, we compared the effect of artesunate on MCF-7 cells, MCF-7/ADR cells, A549 cells, A549/DDP cells, and A549/TAX cells (Fig. 4h, see also Fig. S1a and S1e). The data showed that artesunate killed the A549/TAX cells with greater efficiency than it killed the A549 cells or A549/DDP cells (Fig. S1e and Fig. 4h). In addition, we found that the lysosomal cathepsin activity in A549/TAX cells was significantly enhanced compared with that in the control cells (see Fig. 1b–c). On the other hand, artesunate had similar effects on the proliferation of the MCF-7 cells and MCF-7/ADR cells (Fig. S1a and Fig. 4h), and this was consistent with the levels of lysosomal activity in the two cell types (see Fig. 1e). These findings suggest that artesunate exerts a greater cytotoxic effect on cancer cells with higher lysosomal enzyme activity.

Inhibition of lysosomal function enhances the cytotoxicity of artesunate in A549/TAX cells

CQ is an approved antimalarial drug that blocks lysosomal activity, leading to cell death [25]. Our results showed that CQ inhibited the proliferation of A549/TAX cells (Fig. 5a) and the activity of lysosomal enzymes (Fig. 5b). Interestingly, CQ sensitized the cells to artesunate treatment. Upon treatment with CQ, artesunate effectively killed the cells at lower doses than it did without CQ

pretreatment (Fig. 5c). In addition, Western blot analysis results showed that CQ enhanced the artesunate-induced inhibition of lysosomal protein expression levels (Fig. 5d).

In addition, knocking down TFEB decreased the levels of cathepsin L in the A549/TAX cells (Fig. 5e) and sensitized these cells to artesunate treatment (Fig. 5f). Collectively, these results suggest that lysosomal inhibition was critical for the death of the A549/TAX cells induced by artesunate/CQ treatment, and the inhibition of lysosomal function by CQ potentiated the cytotoxic effect of artesunate to kill the A549/TAX cells.

ROS production contributes to lysosomal inhibition and the cytotoxicity of artesunate in A549/TAX cells

Artemisinin contains an endoperoxide moiety that reacts with iron to produce toxic ROS, and the accumulation of ROS can lead to the initiation of cell death. Therefore, we reasoned that the toxic effect of artesunate on tumor cells may be attributed to ROS production. We measured the levels of ROS with DHE, an oxidation-sensitive fluorescent dye, in the A549/TAX cells. Indeed, the levels of ROS were significantly increased after artesunate treatment in a dose-dependent manner, and the effect was partially reversed by the addition of *N*-acetyl-L-cysteine (NAC), a common ROS scavenger (Fig. 6a). The fluorescence intensity of LysoSensor in the A549/TAX cells was decreased upon artesunate treatment, and the addition of NAC partially restored the LysoSensor fluorescence signal intensity (Fig. 6b). To determine the role of ROS in lysosomal function, cells were cotreated with TX, a water-soluble vitamin E analog and potent scavenger of the hydroxyl radical. Our data showed that TX reversed the inhibition

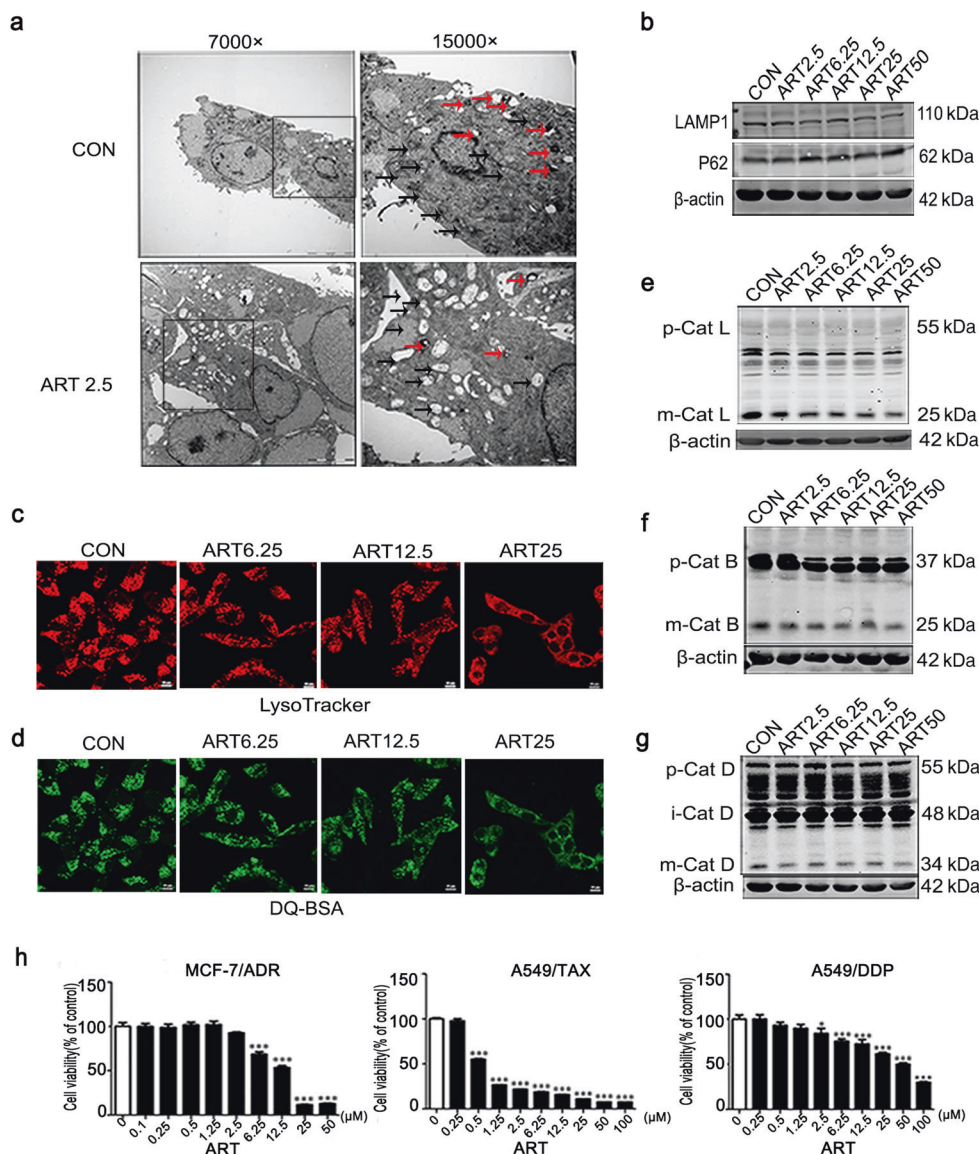


Fig. 4 Artesunate inhibits the function of lysosomes in A549/TAX cells in a dose-dependent manner. **a** Electron microscopy image of the A549/TAX cells treated with artesunate for 24 h. The black arrow indicates mitochondria, and the red arrow indicates lysosomes. **b** Western blot detection of LAMP1 and P62 in the A549/TAX cells after treatment with artesunate for 24 h. Actin was used as the loading control. **c** LysoTracker detection in the A549/TAX cells after treatment with different concentrations of artesunate for 24 h. **d** DQ Green BSA results showing the activity in the A549/TAX cells of lysosomal enzymes after treatment with artesunate for 24 h. Western blot detection of cathepsin L (**e**), cathepsin B (**f**), and cathepsin D (**g**) in the A549/TAX cells after treatment with artesunate in different concentration for 24 h. **h** CCK-8 results showing the effect of artesunate on the A549/DDP, MCF-7/ADR, and A549/TAX cells. Actin was used as the loading control. Values are presented as the means \pm SD from three independent experiments. * $P < 0.05$, *** $P < 0.001$, and ns $P > 0.05$ versus the control group.

of lysosomal enzymes (mature cathepsin L) that had been induced by artesunate (Fig. 6c) and weakened artesunate-induced cell death (Fig. 6d).

DISCUSSION

With an increase in the research on autophagy, lysosomal function, in the last step of the autophagy process, has become a new research topic. The lysosome is not only a waste disposal system that maintains the cell internal environment but also an important component of signal transduction pathways [6]. Recently, increasing evidence has shown that lysosomes participate in cancer cell death and drug resistance [26–28].

The activity and expression levels of cathepsin B, cathepsin D, and cathepsin L increase in various tumor cells, such as those of breast cancer, ovarian cancer, cervical cancer, colon cancer, and lung cancer [29–31]. The secretion of enzymatically inactive pro-cathepsin D enhances lung cancer cell growth [31]. Proteolytic interactions affect cancer cell signaling and play roles in tumor invasion and metastasis [32, 33]. Cathepsin L is involved in ionizing radiation-induced epithelial–mesenchymal transition and in increased glioma invasion and migration by translocating to the nucleus and activating the Smad pathway [34]. A few studies have also shown that the release of lysosomal enzymes may promote cell apoptosis [28, 35–38]. Furthermore, a massive release of cathepsins from lysosomes is related to tumor invasion

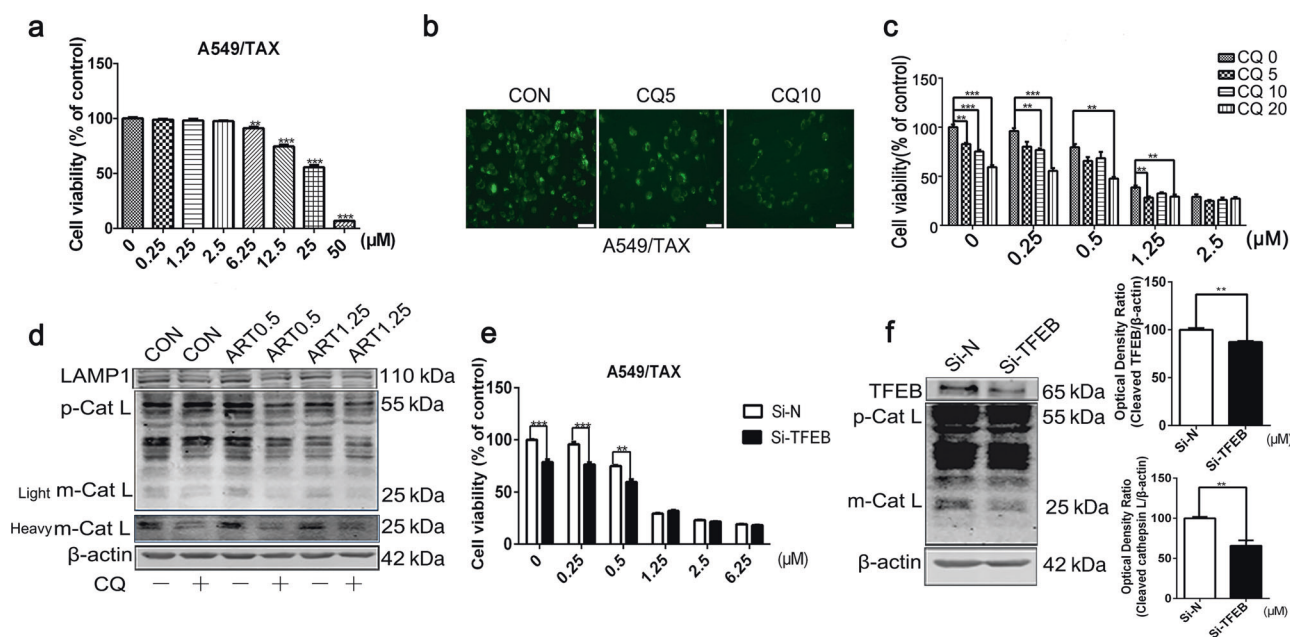


Fig. 5 Inhibition of lysosomal function enhances the cytotoxicity induced by artesunate in A549/TAX cells. **a** CCK-8 results showing proliferation levels of the A549/TAX cells treated with CQ for 72 h. **b** DQ Green BSA results showing the activity of lysosomal enzymes in the A549/TAX cells after treatment with CQ for 24 h. **c** CCK-8 results showing TAX/A549 cells proliferation after artesunate and CQ treatment. **d** Western blot detection of LAMP1 and Cathepsin L in the A549/TAX cells treated with artesunate for 24 h in the presence or absence of CQ. Actin was used as the loading control. **e** CCK-8 results showing the proliferation of the TFEB-knockdown cells treated with artesunate for 72 h. **f** Western blot detection of TFEB and Cathepsin L in the Si-TFEB-A549/TAX cells. Values are presented as means \pm SD from three independent experiments. $^{**}P < 0.01$, $^{***}P < 0.001$, and $^{ns}P > 0.05$ versus the control group.

and metastasis [39]. Thus, cathepsins play major roles in the proliferation and death of cancer cells. The distribution and different forms of cathepsins affect their functions, and the relationship between the function of cathepsins and cell survival deserves further study. In this research, we focused on the proteolytic effect of cathepsins in lysosomes, which represents lysosomal function. We found that artesunate decreased the level of maturation cathepsins.

A recent study showed that lysosomal function is associated with drug resistance. Fluorouracil efficiency in the treatment of colorectal cancer was limited by drug resistance. ABHD5, also known as alpha-beta hydrolase domain-containing 5 (CGI-58), is located on the lysosome. Ou et al. found that ABHD5 enhanced lysosomal function and increased uracil yield from lysosomes; therefore, the uptake of fluorouracil as an exogenous uracil decreased, which enhanced cell resistance to fluorouracil. In addition, ABHD5 deficiency impaired the uracil yield and therefore increased the uptake of fluorouracil, which augmented cell sensitivity to fluorouracil [40].

In our research, we also found that enhanced lysosomal function was associated with drug resistance. We found that two drug-resistant A549 cell lines had enhanced lysosomal function compared with that in normal A549 cells. We also found that TFEB overexpression promoted cell resistance to chemotherapeutic treatment and that TFEB knockdown increased cell sensitivity to the treatment. Upregulated Cathepsin L also induced epithelial-mesenchymal transformation, which caused drug resistance in cancer cells [41]. Therefore, drugs that inhibit the function of lysosomes or cathepsins are likely to inhibit the emergence of drug resistance in tumor cells. In addition, we found that artesunate significantly increased the pH of lysosomes and reduced the levels of proenzyme and mature cathepsins. In particular, artesunate was more lethal to cancer cells that had relatively high lysosomal enzyme activity. Our findings reveal, for the first time, a novel role for artesunate in

inhibiting lysosomal function, highlighting the significance of artesunate in chemotherapy.

However, we also acknowledge conflicting data from Yang's work. Yang reported that artesunate-induced cell death in human cancer cells by enhancing lysosomal function [42]. Artesunate reported in the Yang article was coupled with a fluorescent group, which may have affected the results. The molecular weight of the fluorescent group was >300 Da, which is larger than artesunate itself. The autophagy/lysosomal pathway is greatly affected by different physiological or pathological conditions. In addition, it is possible that the types of cells we used were different than those used by Yang; thus, the autophagy/lysosomal activity and other physiological characteristics may have been different. HeLa cells and HepG2 cells were used in Yang's study, whereas A549 cells and MCF-7 cells were used in our research.

Mitochondria are important sources of ROS in cells. As the terminal electron acceptor in the respiratory chain [43], oxygen is involved in the oxidative phosphorylation of ATP, which is of great significance. In a biological context, ROS are formed as a natural byproduct of the normal metabolism of oxygen and have important roles in cell signaling and homeostasis. However, excessive levels of ROS can damage the mitochondria. When ROS levels increase to a threshold level, they will activate the nonspecific mitochondrial permeability transition pore to open, thereby reducing the mitochondrial membrane potential (MMP) and inducing the release of cytochrome c into the cytoplasm, ultimately triggering apoptosis [44]. It was also found in our study that, after artesunate treatment, there was a significant increase in mitochondrial vacuolation and a decrease in MMP in the tumor cells, as well as the level of cleaved PARP. The dysfunction induced in lysosomes by artesunate also decreased their ability to scavenge abnormal mitochondria, increasing the cell death rate.

This study aimed to explore the effect of artesunate on lysosomal function in drug-resistant cells and its relationship with cell death. The inhibition of lysosomal function may be one of the

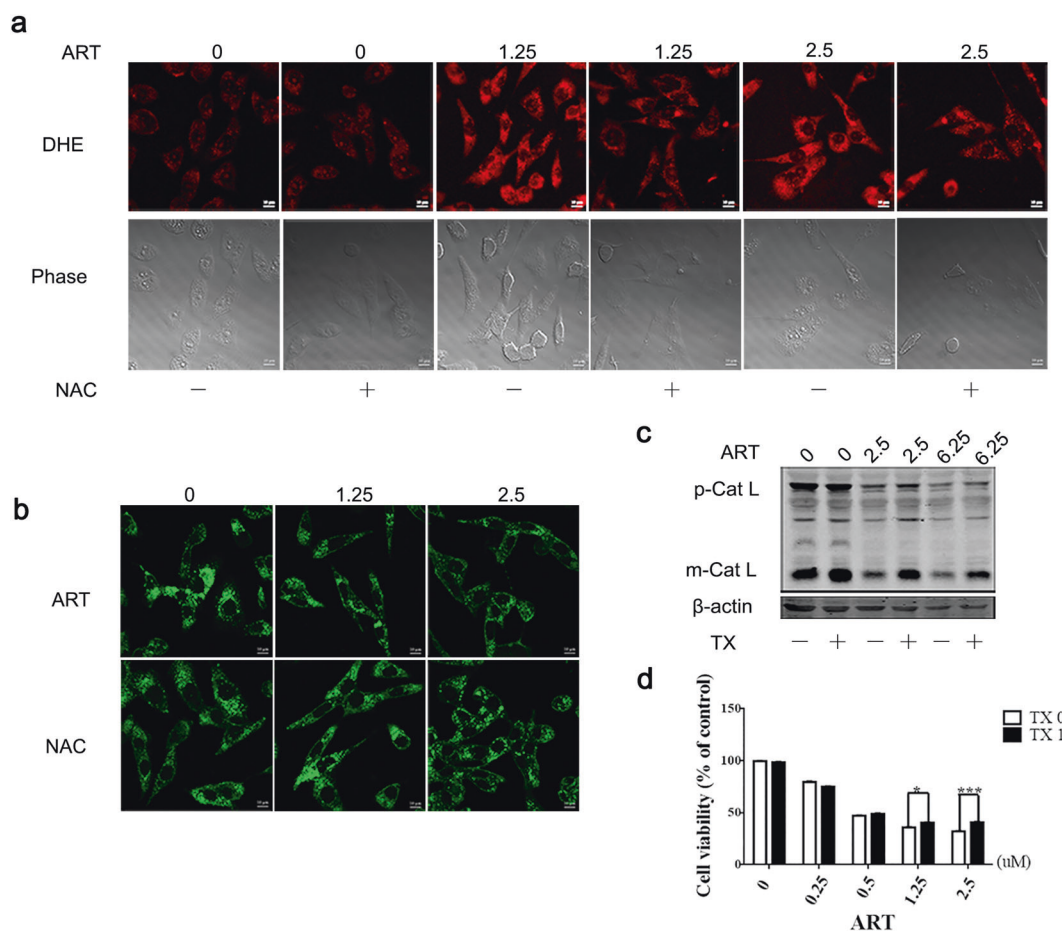


Fig. 6 Artesunate inhibits cell proliferation by inhibiting lysosomal function partly through ROS. **a** DHE results showing the ROS level in the A549/TAX cells treated with artesunate for 24 h in the presence or absence of NAC. **b** LysoSensor results showing the effect of NAC on the A549/TAX cells treated with artesunate for 24 h. **c** Western blot detection of Cathepsin L in the cells treated with artesunate and TX. **d** CCK-8 results showing the effect of TX on the MCF-7/ADR cells treated with artesunate for 72 h. Values are presented as the means \pm SD from three independent experiments. * $P < 0.05$, *** $P < 0.001$, and ns $P > 0.05$ versus the control group.

mechanisms by which cytotoxicity is generated by chemotherapy drugs, which is especially important for drug-resistant cells with high lysosomal activity. This study provides the theoretical foundation and experimental evidence for improving the efficacy of chemotherapy in malignant tumors.

ACKNOWLEDGEMENTS

This work was supported by grants from the Natural Science Foundation of Jiangsu Province (No. BK20151233), the Scientific and Technological Innovation Team Building Program of Suzhou Vocational Health College (SZWZYTD201801), the Youth Project of Health and Family Planning Bureau of Suzhou New District (No. 2017Q005), Suzhou industrial technology innovation (No. SYSD2016062), the Priority Academic Program Development of the Jiangsu Higher Education Institutes (PAPD).

AUTHOR CONTRIBUTIONS

ZL completed most of the research work; YTZ and MX performed some research work and wrote the paper. JLQ provided suggestions for the research. SQL and FL designed the research work and revised the paper.

ADDITIONAL INFORMATION

The online version of this article (<https://doi.org/10.1038/s41401-020-0445-z>) contains supplementary material, which is available to authorized users.

Competing interests: The authors declare no competing interests.

REFERENCES

- Tredan O, Galmarini CM, Patel K, Tannock IF. Drug resistance and the solid tumor microenvironment. *J Natl Cancer Inst.* 2007;99:1441–54.
- Housman G, Byler S, Heerboth S, Lapinska K, Longacre M, Snyder N, et al. Drug resistance in cancer: an overview. *Cancers.* 2014;6:1769–92.
- Shiraishi N, Akiyama S, Kobayashi M, Kuwano M. Lysosomotropic agents reverse multiple drug resistance in human cancer cells. *Cancer Lett.* 1986;30:251–9.
- Rios-Luci C, Garcia-Alonso S, Diaz-Rodriguez E, Nadal-Serrano M, Arribas J, Ocana A, et al. Resistance to the antibody-drug conjugate T-DM1 is based in a reduction in lysosomal proteolytic activity. *Cancer Res.* 2017;77:4639–51.
- Appelqvist H, Waster P, Kagedal K, Ollinger K. The lysosome: from waste bag to potential therapeutic target. *J Mol Cell Biol.* 2013;5:214–26.
- de Duve C. The lysosome turns fifty. *Nat Cell Biol.* 2005;7:847–9.
- Ohkuma S, Moriyama Y, Takano T. Identification and characterization of a proton pump on lysosomes by fluorescein-isothiocyanate-dextran fluorescence. *Proc Natl Acad Sci USA.* 1982;79:2758–62.
- Bucci C, Thomsen P, Nicoziani P, McCarthy J, van Deurs B. Rab7: a key to lysosome biogenesis. *Mol Biol Cell.* 2000;11:467–80.
- Brown MS, Goldstein JL. A receptor-mediated pathway for cholesterol homeostasis. *Science.* 1986;232:34–47.
- Boya P. Lysosomal function and dysfunction: mechanism and disease. *Antioxid Redox Signal.* 2012;17:766–74.
- Kallifatidis G, Hoepfner D, Jaeg T, Guzman EA, Wright AE. The marine natural product manzamine A targets vacuolar ATPases and inhibits autophagy in pancreatic cancer cells. *Mar Drugs.* 2013;11:3500–16.
- Zhitomirsky B, Assaraf YG. Lysosomal sequestration of hydrophobic weak base chemotherapeutics triggers lysosomal biogenesis and lysosome-dependent cancer multidrug resistance. *Oncotarget.* 2015;6:1143–56.

13. Kumar B, Kalvala A, Chu S, Rosen S, Forman SJ, Marcucci G, et al. Antileukemic activity and cellular effects of the antimalarial agent artesunate in acute myeloid leukemia. *Leuk Res.* 2017;59:124–35.
14. Vandewynckel YP, Laukens D, Geerts A, Vanhove C, Descamps B, Colle I, et al. Therapeutic effects of artesunate in hepatocellular carcinoma: repurposing an ancient antimalarial agent. *Eur J Gastroenterol Hepatol.* 2014;26:861–70.
15. Augustin Y, Krishna S, Kumar D, Pantziarka P. The wisdom of crowds and the repurposing of artesunate as an anticancer drug. *Ecancermedalscience.* 2015;9:ed50.
16. Zhou C, Pan W, Wang XP, Chen TS. Artesunate induces apoptosis via a Bak-mediated caspase-independent intrinsic pathway in human lung adenocarcinoma cells. *J Cell Physiol.* 2012;227:3778–86.
17. Berdelle N, Nikolova T, Quiros S, Efferth T, Kaina B. Artesunate induces oxidative DNA damage, sustained DNA double-strand breaks, and the ATM/ATR damage response in cancer cells. *Mol Cancer Ther.* 2011;10:2224–33.
18. Beccafico S, Morozzi G, Marchetti MC, Riccardi C, Sidoni A, Donato R, et al. Artesunate induces ROS- and p38 MAPK-mediated apoptosis and counteracts tumor growth in vivo in embryonal rhabdomyosarcoma cells. *Carcinogenesis.* 2015;36:1071–83.
19. Button RW, Lin F, Ercolano E, Vincent JH, Hu B, Hanemann CO, et al. Artesunate induces necrotic cell death in schwannoma cells. *Cell Death Dis.* 2014;5:e1466.
20. Marwaha R, Sharma M, DQ-Red BSA. Trafficking assay in cultured cells to assess cargo delivery to lysosomes. *Bio Protoc.* 2017;7:e2571.
21. Greenshields AL, Fernando W, Hoskin DW. The anti-malarial drug artesunate causes cell cycle arrest and apoptosis of triple-negative MDA-MB-468 and HER2-enriched SK-BR-3 breast cancer cells. *Exp Mol Pathol.* 2019;107:10–22.
22. Jing W, Dong H, Min M, Runpeng Z, Xuwei X, Ru C, et al. Dependence of artesunate on long noncoding RNA-RP11 to inhibit epithelial-mesenchymal transition of hepatocellular carcinoma. *J Cell Biochem.* 2019;120:6026–34.
23. DeVorkin L, Gorski SM. LysoTracker staining to aid in monitoring autophagy in *Drosophila*. *Cold Spring Harb Protoc.* 2014;2014:951–8.
24. Button RW, Roberts SL, Willis TL, Hanemann CO, Luo S. Accumulation of autophagosomes confers cytotoxicity. *J Biol Chem.* 2017;292:13599–614.
25. Mauthe M, Orhon I, Rocchi C, Zhou X, Luhr M, Hijlkema KJ, et al. Chloroquine inhibits autophagic flux by decreasing autophagosome-lysosome fusion. *Autophagy.* 2018;14:1435–55.
26. Piao S, Amaravadi RK. Targeting the lysosome in cancer. *Ann N Y Acad Sci.* 2016;1371:45–54.
27. Kallunki T, Olsen OD, Jaattela M. Cancer-associated lysosomal changes: friends or foes? *Oncogene.* 2013;32:1995–2004.
28. Fehrenbacher N, Gyrd-Hansen M, Poulsen B, Felbor U, Kallunki T, Boes M, et al. Sensitization to the lysosomal cell death pathway upon immortalization and transformation. *Cancer Res.* 2004;64:5301–10.
29. Rochefort H, Garcia M, Glondu M, Laurent V, Liaudet E, Rey JM, et al. Cathepsin D in breast cancer: mechanisms and clinical applications, a 1999 overview. *Clin Chim Acta.* 2000;291:157–70.
30. Winiarski BK, Wolanska KI, Rai S, Ahmed T, Acheson N, Gutowski NJ, et al. Epithelial ovarian cancer-induced angiogenic phenotype of human omental microvascular endothelial cells may occur independently of VEGF signaling. *Transl Oncol.* 2013;6:703–14.
31. Vetvicka V, Vetvickova J, Benes P. Role of enzymatically inactive procathepsin D in lung cancer. *Anticancer Res.* 2004;24:2739–43.
32. Joyce JA, Pollard JW. Microenvironmental regulation of metastasis. *Nat Rev Cancer.* 2009;9:239–52.
33. Mason SD, Joyce JA. Proteolytic networks in cancer. *Trends Cell Biol.* 2011;21:228–37.
34. Fei Y, Xiong Y, Shen X, Zhao Y, Zhu Y, Wang L, et al. Cathepsin L promotes ionizing radiation-induced U251 glioma cell migration and invasion through regulating the GSK-3beta/CUX1 pathway. *Cell Signal.* 2018;44:62–71.
35. Foghsgaard L, Wissing D, Mauch D, Lademann U, Bastholm L, Boes M, et al. Cathepsin B acts as a dominant execution protease in tumor cell apoptosis induced by tumor necrosis factor. *J Cell Biol.* 2001;153:999–1010.
36. Guicciardi ME, Deussing J, Miyoshi H, Bronk SF, Svingen PA, Peters C, et al. Cathepsin B contributes to TNF-alpha-mediated hepatocyte apoptosis by promoting mitochondrial release of cytochrome c. *J Clin Invest.* 2000;106:1127–37.
37. Leist M, Jaattela M. Four deaths and a funeral: from caspases to alternative mechanisms. *Nat Rev Mol Cell Biol.* 2001;2:589–98.
38. Serrano-Puebla A, Boya P. Lysosomal membrane permeabilization in cell death: new evidence and implications for health and disease. *Ann N Y Acad Sci.* 2016;1371:30–44.
39. Messner B, Ploner C, Laufer G, Bernhard D. Cadmium activates a programmed, lysosomal membrane permeabilization-dependent necrosis pathway. *Toxicol Lett.* 2012;212:268–75.
40. Ou J, Peng Y, Yang W, Zhang Y, Hao J, Li F, et al. ABHD5 blunts the sensitivity of colorectal cancer to fluorouracil via promoting autophagic uracil yield. *Nat Commun.* 2019;10:1078.
41. Bao J, Zheng L, Zhang Q, Li X, Zhang X, Li Z, et al. Deacetylation of TFEB promotes fibrillar Abeta degradation by upregulating lysosomal biogenesis in microglia. *Protein Cell.* 2016;7:417–33.
42. Yang ND, Tan SH, Ng S, Shi Y, Zhou J, Tan KS, et al. Artesunate induces cell death in human cancer cells via enhancing lysosomal function and lysosomal degradation of ferritin. *J Biol Chem.* 2014;289:33425–41.
43. Skulachev VP. Role of uncoupled and non-coupled oxidations in maintenance of safely low levels of oxygen and its one-electron reductants. *Q Rev Biophys.* 1996;29:169–202.
44. Lenaz G. Mitochondria and reactive oxygen species. Which role in physiology and pathology? *Adv Exp Med Biol.* 2012;942:93–136.